The influence of experimental bioactive glasses on pulp cells behavior in vitro

Caroline Mocquot, Pierre Colon, Delihta Fernando, Phil Jackson, Nelly Pradelle-Plasse, Brigitte Grosgogeat, Nina Attik

▶ **To cite this version:**

Caroline Mocquot, Pierre Colon, Delihta Fernando, Phil Jackson, Nelly Pradelle-Plasse, et al.. The influence of experimental bioactive glasses on pulp cells behavior in vitro. Dental Materials, 2020, 36, pp.1322 - 1331. 10.1016/j.dental.2020.07.006 . hal-03492416

HAL Id: hal-03492416
https://hal.science/hal-03492416v1

Submitted on 17 Oct 2022

HAL is a multi-disciplinary open access archive for the deposit and dissemination of scientific research documents, whether they are published or not. The documents may come from teaching and research institutions in France or abroad, or from public or private research centers.

L'archive ouverte pluridisciplinaire **HAL**, est destinée au dépôt et à la diffusion de documents scientifiques de niveau recherche, publiés ou non, émanant des établissements d'enseignement et de recherche français ou étrangers, des laboratoires publics ou privés.

Distributed under a Creative Commons Attribution - NonCommercial 4.0 International License

Version of Record: https://www.sciencedirect.com/science/article/pii/S0109564120301937
Manuscript_b68cc0235abce9d517fbbd8a2cc6904a

THE INFUENCE OF EXPERIMENTAL BIOACTIVE GLASSES ON PULP CELLS BEHAVIOR *IN VITRO*

Caroline Mocquot[a,b], Pierre Colon[a,b], Delihta Fernando[a], Phil Jackson[c], Nelly Pradelle-Plasse[a,b], Brigitte Grosgogeat[a,d,e], Nina Attik[a,d]

[a] *1Université de Lyon* - Université Claude Bernard Lyon 1, *UMR CNRS 5615, Laboratoire des Multimatériaux et Interfaces, F-69622 Villeurbanne, France*

[b] Département d'Odontologie Conservatrice - Endodontie. Université de Paris, Faculté dentaire, Hôpital Rothschild, Assistance Publique-Hôpitaux de Paris, France
[c] Lucideon Inc., Penkhull, Stoke-On-Trent ST4 7LQ, UK.
[d] Université de Lyon, Université Claude Bernard Lyon 1, Faculté d'Odontologie, 69008 Lyon, France
[e] Hospices civils de Lyon, Service d'0dontologie, 69007 Lyon, France

* Corresponding author: Dr Nina ATTIK, LMI/ Faculté d'Odontologie
11 rue Guillaume Paradin 69372 LYON Cedex 08, FRANCE nina.attik@univ-kyon1.fr

© 2020 published by Elsevier. This manuscript is made available under the CC BY NC user license
https://creativecommons.org/licenses/by-nc/4.0/

1. Introduction

Carious disease is still a neglected topic despite the acknowledgment of the WHO that it is still a major health problem in most industrialized countries. Report highlights that 60-90 percent of children and the vast majority of adults are affected by dental caries [1,2]. Erosion (a non-bacteria-mediated process) and carious lesions are the two main consequences of tooth demineralization resulting in the mineral structures loss of the enamel and dentin tissues [3]. Moreover, dental erosion prevalence is increasing steadily [4,5]. The approach of restorative dentistry has significantly changed recently: surgical strategies are decreasing in favor of biological approaches based on preventive dentistry and minimal or non-invasive options [6,7]. Mineral ions from hydroxyapatite crystals (HA) present in enamel and dentin are removed due to acidic attack (erosive and/or carious lesions), resulting in the process of demineralization. Remineralization is a non-invasive treatment used to regenerate mineralized tissues after demineralization [3]. Remineralization may occur with a dissolution / re-precipitation process in enamel or dentin although stimulation of pulp cells could also evoke tertiary dentin deposition along the walls of the pulpal chamber [8-11].

Bioactive glasses were initially used for medical application due to their ability to form a bond with bone tissue [12]. Some products containing BAG particles are already available in the market such as bone filling materials (Biogran® - Perioglas®). Besides bone regeneration, bioactive glass has found its niche in dentistry. Novamin® and BiominF® are two examples of recently developed toothpastes containing BAG (with or without Fluor) for enamel remineralization and dental hypersensitivity. Finally, BAG particles are used for air-abrasion

(ProSylc (Novamin®) [13]. Research is also focused on using bioactive glasses in air polishing - techniques to stimulate mineralization of tooth tissue through apatite formation [14-16]. The first BAG was made in 1969 by professor Larry Hench (BAG 45S5). The composition was: 45% Silicon Oxide (SiO_2) – 24.5% Calcium Oxide (CaO) - 24.5% Sodium Oxide (Na_2O) – 6% Phosphorus Oxide (P_2O_5). The original composition (45S5) and manufacturing methodology for BAG are modified to create mesoporous BAG, to change particle size (nano or micro-scale) or to introduce additives. In a previous study, experimental BAG have been developed (0NaMBG) by our group. The typical composition of these particles is without sodium. The enhanced fluxing in compositions with high sodium affects the textural features by reducing the porosity due to fusion of pores. Therefore, the porosity increases with increasing calcium oxide as opposed to sodium oxide [17]. The porosity is an interesting property to enhance surface area and therefore the bioactivity of particles [18].

The use of BAGs as pulp capping materials has been applied over many years [19]. Currently biomaterials with BAG are not yet commercially available for this application. Therefore, development of *in vitro* studies to assess the effects of BAG on human dental pulp cells (hDPCs) is fundamental. In this context, the development of bioactive materials, as BAG, for pulp regeneration is an interesting perspective [8,20]. Human dental pulp cells may represent a different population of differentiated and undifferentiated cells with great potential for pulp tissue and dentin regeneration. They can be successfully used to evaluate new biomaterials for different dental applications [21]. The primary pulp function is dentin formation, which begins at the moment that the peripheral mesenchymal cells differentiate into odontoblasts and start the deposition of the collagen matrix, in a mineralization process resulting in the complete tooth formation [22].

In this study, we aimed to assess the effects of fine and large 0NaMBG particles on biocompatibility and mineralization ability of human dental pulp cells. The investigated 0NaMBG particles composition has been defined as $75SiO_2$:15CaO:$0Na_2O$:$10P_2O_5$ and it has been synthesised using an acid catalysed sol–gel assisted method [17]. Therefore, we evaluated the influence of particles size and surface area for a given composition of sol-gel bioactive glasses on pulp cells behavior (cell metabolic activity, cell morphology, viability, ALP activity, and mineralization ability). Two hypotheses were suggested (1) both large and fine 0NaMBG particles would enhance pulp cells behavior; (2) a very high surface area of the investigated large particles would better improve the dental pulp cells behavior than the fine particles.

.

2. Materials and methods

2.1 Bioactive glass synthesis and characterization

0NaMBG particles with 75%SiO_2, 15%CaO, 0%Na_2O and 10%P_2O_5 composition were synthesized by an acid catalyzed sol-gel method assisted by an evaporation-induced self-assembly (EISA) process [17]. Tetraethyl orthosilicate (TEOS), Triethyl phosphate (TEP) and calcium acetate monohydrate were used as precursors. The temperature of drying and calcination was 60°C and 310°C, respectively. The particles were characterized by X-ray fluorescence (XRF), X-ray diffractometer (XRD), Brunauer-Emmett-Teller (BET/BJH), Fourier Transform Infra-Red Spectroscopy (FTIR), Scanning Electron Microscopy (SEM), Transmission Electron Microscopy (TEM) and Inductive Coupled Plasma Spectrometry (ICP) [17]. Two sizes of 0NaMBG were obtained: large (LP) and fine (FP). 90% of large particles were less than 623 µm (D90), 50% were less than 177 µm (D50) and 10% were less than 18 µm (D10) (Table 1).

90% of fine particles were less than 2.97 µm (D90), 50% were is less than 0.157 µm (D50) and 10% were less than 0.003 µm (D10) (Table 1). As shown in table 1, large particles have a higher surface area and pore volume and lower pore size than fine particles. According to the results of our previous study [17], large particles released Ca^{2+} (day 1: 50 ppm – day 3: 70 ppm – Day 7: 80 ppm) as revealed by inductive coupled plasma spectrometry after immersion in deionised water. Before cell contact, the samples were sterilized under UV for 30 minutes after which they were suspended in the culture media at a concentration of 800 µg/ml. Preliminary assays have been carried out to determine the most efficient concentration in the current experimental conditions (data not shown).

2.2 Cell culture

Dental Pulp cells (hDPCs cells) were isolated and harvested from the pulp of sound human third molar germ (14–16 years old) extracted for orthodontic reasons. Informed consent was obtained from the patients at the University of Lyon 1 – Hospices civils of Lyon (HCL), France. The culture protocol was carried out using a modification method of Couble et al. 2000 [23]. Whole pulps (15 specimens) were separated from the crowns and roots and removed through the developing apical end, except the apical part of the pulps to prevent periodontal fibroblast contamination. Selected specimens were minced into small explants and were grown on 35 mm diameter EASY GRIP culture dishes (Thermo Scientific France). They were cultured in Basel Medium Eagle (BME) with 10% fetal bovine serum, 1% of vitamin C, 2% penicillin/streptomycin, and 1% amphotericin B. Cultures were maintained at 37°C under a humidified atmosphere of 5% CO_2 in air for 4-7 weeks. The medium associated with the generated cells was changed every 2 days, and cells were passaged after 5 days of culture. After reaching confluence, cells were trypsinized and resuspended in the culture medium**.** Cell cultures were examined routinely under an inverted microscope.

In this study, cells were placed in indirect contact with 0NaMBG. In the indirect contact the samples (concentration 800 µg/ml) are immersed in culture media for 24h and the ion extracts are collected and contacted with cells for the evaluations [24,25].

2.3 Alamar blue – metabolic activity

Cell metabolic activity was quantified using Alamar Blue assay. Alamar blue® solution (DAL1025, Thermo Scientific France) was used in this study. The assay was carried out using a modification method of McNicholl et al. [26]. Briefly, a 24-microwell plate was used as a 'feeder tray' in which 1mL of cell suspension 10^4 cells/ml was seeded overnight, then exposed to the extract of bioactive glass particles (indirect contact, as described above) for 1, 2 and 3 days. Unexposed control cultures were maintained in the same conditions. Alamar Blue solution was added directly into wells at the final concentration of 10% (v/v) and plates were incubated at 37°C for 4 h without shaking. The amount of Resorufin formed was determined by measuring the absorbance at 570 and 600 nm using a micro-plate reader (Infinite® M 200 PRO, NanoQuant plate, Tecan, France). For each treatment, four wells were analyzed with three independent experiments carried out. The results were expressed as percentage of viability, of the untreated control (100%).

2.4 Quantitative assay of ALP activity

The kit K412-500 was used according to the manufacturer's instructions (BioVision Incorporated, USA). The hDPCs were seeded at a density of 10^4 cells/ml into 24-well plates and were cultured for 7 days in indirect contact with (i) FP, LP 0NaMBG at a concentration of 800 µg/ml and (ii) a control group (cells with culture media and without any particles extracts). Alkaline phosphatase (ALP) activity was measured by adding 50 µL (at the concentration of 5 mM) of ALP reaction solution (2 4-nitropheyl-phosphate disodium salt hexahydrate tablets dissolved in 5,4 ml ALP Assay Buffer) to cell lysate, incubated in the dark

at 37°C for 1 h. Afterwards, the reaction was stopped by adding 20 µl of Stop solution. Then, the absorbance of the resultant colored reaction product pNPP, within the supernatant was measured at 405 nm using a micro-plate reader (Infinite® M 200 PRO, NanoQuant plate, Tecan, France). Finally, ALP activity was calculated according to the following equation:

ALP activity = ([pNPP] (µmol)/ΔT (min) x (ml) x D (dilution factor)

ΔT= reaction time and V (initial voulme added to each well)

2.5 Crystal violet (CV) staining

Cell cytotoxicity was also measured (after 72h of particles extracts contact) using crystal violet staining and colorimetric assay (K329-1000, Biovision, France). After 72h in contact with 0,5% DMSO and with 3 µL of 20 mM doxorubicin for inhibitor controls, fixed cells were rinsed with wash buffer 1 X and stained with 200 µL crystal violet with 20% methanol per well for 20 min at room temperature (RT). Before visualization, the unbound stains were removed by five washes with buffer. Cells were solubilized by adding 300 µL solubilisation solution per well and leaving for 20 min at room temperature on a shaker. The absorbance was measured at 595 nm. Cell viability was calculated as percentage of cytotoxicity using the following formula:

% cytotoxicity: [(OD DMSO - OD sample)/OD DMSO] x100.

2.6 Cell morphology spreading by ConfocaL Laser Scanning Microscopy (CLSM)

Fluorescence staining was performed to observe the formation and the organization of stress fibers and morphological changes. Cells were seeded on a µ_dish glass bottom chamber (Ibidi GmbH, Germany) placed in a complete medium and incubated at 37ºC at a density of 10^4cells/ml for 24 h. The culture medium was replaced with the corresponding extract and incubated again at 37°C for 24 h. Cells were harvested and washed three times

with PBS. Then the cells were fixed for 30 min by incubating in 3.7% formaldehyde in PBS followed by further washing. The cells were permeabilized with 1% Triton X100 in PBS and then blocked with 1% bovine serum albumin in PBS. Actin microfilaments were stained by Alexa Fluor® 488 phalloidin (green fluorescence) at a 1: 100 ratio to visualize pulp cell actin-filaments. Cell nuclei were identified using Propidium Iodide (red fluorescence) at a 1:3000 ratio at room temperature. Supercontinuum white light laser was used to excite Alexa Fluor 488 and Propidium Iodide. Acquisitions were collected sequentially (green fluorescence/red fluorescence) to avoid potential cross-talking between the two channels. The resulting stained cells on the glass bottom chamber in 1% bovine serum albumin in PBS were examined under a Confocal Lase Scanning Microscope CLSM LEICA SP5 X (Leica, Wetzlar, Germany).

2.7 Alizarin red S staining - mineralization

Alizarin red S staining was used to assess matrix mineralization. After Treatment, HDPCs were fixed using formaldehyde (3,7 %, 30 min) and washed with deionized water. 40mM of alizarin red staining solution (pH 4.2) was then added into the 24-well plates.The cells were incubated at room temperature for 40 min, then washed with deionized water 3 times and viewed under a microscope, with images captured. For quantitative calcium analysis (semi-quantification) of mineralized matrix nodules generated from human pulp cells, the cells were treated with 10% cetylpyridinium chloride solution (Sigma-Aldrich) for 15 min at room temperature to dissolve and release the calcium-combined Alizarin Red S into solution. The OD values were read at 560 nm, which represented the relative quantity of mineralization nodules. The experiments were repeated at least 3 times.

2.8 Odontogenic markers: OPN expression and DMP-1

The evaluation of osteopontin (OPN) and Dentin Matrix Protein 1 (DMP-1) expression was performed following cell exposure to 0NaMBG particles extracts, cells fixation and permeabilization. For these endpoints, OPN staining was performed using Rabbit Anti-Osteopontin Polyclonal Antibody, ALexa Fluor® 555 Conjugated (bs-0019R-A555, CliniSciences, France), diluted 1:200 (40 min of incubation with the cells at room temperature). DMP-1 expression was analyzed using two fluorescents stains. Monoclonal Anti-DMP, antibody (SAB140275-100G) was used as the primary antibody at the dilution ratio 1: 50 (2h at 37°C). This was followed by a second staining using Cyanine 3 (AS008, CliniSciences, France) at 1:100 (1h at 37°C). Subsequently, cell nuclei were identified using Dapi (4',6-diamidino-2-phenylindole) at a 1:3000 ratio at room temperature. The stained cells were observed using the microscope CLSM LEICA SP5 X (Leica, Wetzlar, Germany). Tow laser sources were used to excite the indicated stains: a supercontinuum white light laser and a laser Diode-Pumped Solid-State (405nm).

2.9 Statistical analysis

Data were analyzed using statistical software SPSS™ (V21.0, IBM, IL, USA) and fond to be normally distributed. Non-parametric analysis and multiple comparison were achieved using One-way Analysis of Variance (ANOVA) with a repetition test followed by Post Hoc tests. A comparison was made between the two tested particle groups (fine vs large particles) and exposed cells were compared to control group cells (Fine or Large particles vs controls cells). Results were reported as mean standard deviation (±SD) and statistical significance was accepted at $p < 0.05$.

3 Results

3.1 Cell metabolic activity by Alamar blue assay

Cells were treated with 0NaMBG for 24, 48 and 72 hours. The results of cell metabolic activity comparing the fine and the large particles are shown in **Fig. 1**. At 24 h, the metabolic activity of cells treated with samples were similar to the control cells. No cytotoxic effects were observed for both conditions. Interestingly at day 3, cells treated with particles expressed higher metabolic activity ($p = 0.03$) than the control cells with a significant enhancement for the large particles after 72h of incubation ($p = 0.02$).

3.2 Quantitative assay of ALP activity

Cells were treated with 0NaMBG for 7 days. Both fine and large MBGs particles significantly increased both extra and intra cellular ALP activity ($p = 0.03$). More enhancement was observed with large particles for the extracellular ALP compared with the intracellular ALP, which was significantly higher ($p = 0.01$) in the presence of fine particles **(Fig. 2).**

3.3 Cells viability by Cristal Violet assay

The results of cell cytotoxicity for the different conditions are shown in **Fig. 3,** before solubilisation, and in **Fig. 4** as the percentage of cell viability after the staining solubilisation. The number of adhered cells as well as the cell spreading area were slightly higher in the presence of the particles as shown by Crystal Violet staining **(Fig. 3).** The viability rate was not significantly different between FP and LP ($p=0.28$), and between exposed cells to both particles and controls cells ($p=0.37$). No cytotoxic effect was observed in the presence of tested particles.

3.4 Cells morphology spreading by CLSM

Dental pulp cells exhibited good cytoskeletal architecture as seen from actin cytoskeleton staining. Good cell spreading and adhesion was observed in the presence of fine and large particles extracts **(Fig. 5).**

3.5 Mineralization ability

The mineralization potential of the hDPs cells can be determined from Alizarin Red S staining of evaluated cells following indirect contact with MBGs particles. After 14 days of incubation, both fine and large particles revealed significant enhancement of the extracellular calcium deposition amount **(Fig. 6)** when compared to control cells ($p = 0.02$). Mineralized nodules were noticeable by optical microscopy; Images demonstrated more mineralization nodules when cells are interfaced with both fine and large particles compared to the control cells **(Fig. 7)**. 0NaMBG enhanced mineralization of HDPCs.

3.6 OPN and DMP-1 expression by CLSM using immunofluorescence staining

The staining of OPN was revealed in the cytoplasm (slight red fluorescence) of cells growing in the presences of large particles extracts. Cells were negatively stained for OPN on cells growing in the presence of fine particles extracts similarly to the control cells **(Fig. 8).** However, the staining of DMP-1 was shown in the cytoplasm (intense red fluorescence) of both cells growing in the presences of fine and large particles extracts **(Fig. 9).**

4 DISCUSSION

Pulp tissue vitality preservation and apical periodontitis prevention are part of the minimally invasive biologically-based concept that is key to contemporary clinical endodontic therapies [8]. Bioactive materials, such as bioceramics, are already marketed to be used in vital pulp procedures [27]. MBG appear to be a potential candidate for these procedures [28]. Indeed, MBG presents chemical compositions similar to those of conventional bioactive sol-gel glasses with the added value of an ordered mesoporous arrangement which could possibly contribute to an enhanced bioactive behavior [29]. The ability of mesoporous bioactive glasses to form hydroxyapatite has already been validated [30]. However, to the best of our knowledge, assessment of biocompatibility and bioactivity of mesoporous BAG in contact with dental pulp cells has not been widely studied.

The 0NaMBG used represents experimental bioactive glasses without sodium. The composition of these particles was obtained in our previous sol-gel study investigating the influence of network modifiers and order of precursor addition. The aim was to evaluate the influence of these parameters on the porosity of sol-gel bioactive glasses [17,18]. The composition of BAG: 75%SiO_2, 15%CaO, 0%Na_2O and 10%P_2O_5 was retained because of the higher porosity obtained using increasing calcium oxide as opposed to sodium oxide [17]. The porosity is an interesting property to enhance surface area and therefore the particles

bioactivity. Assessment of experimental particles in contact with cells is a fundamental first step of biocompatibility and bioactivity evaluation. Cell biological assessment should conducted on specific cells according the recommendations established by ISO 10993-5 [31,32].

The larger 0NaMBG particles generated initially were ball milled to reduce the primary particle size and so obtain finer particles. The aim was to achieve a particle size of less than 10 μm that could be used as filler in dental adhesives [10]. According to Gjorgievska et al. [33] particle size is a major parameter with diameters of 700 μm being suitable for use as bone substitutes, but too large for dental applications. In this case, a more appropriate size would be less than 90 μm.

In a pilot study, we used primary human gingival fibroblasts (HGF) and cementoblast cells to assess the cytocompatibility and mineralization ability of the developed 0NaMBGs. The positive results obtained convinced us to use Human dental Pulp cells (hDPCs) that are more related to the clinical situation and more sensitive than HGF and cementoblasts cells. Moreover, the use of hDPCs to assess the mineralization ability and biocompatibility *in vitro,* is more relevant to BAG restorative or endodontic applications. Indeed, hDPCs have been found to promote dental pulp repair and regeneration via synthesis of extracellular matrix to form the reparative dentin [34,35]. In most clinical situations, BAGs are not in direct contact with cells, but their extracts could reach target cells. Hence, the extraction technique, an indirect contact method, is widely used when assessing the cytocompatibility of dental materials [36]. It could be interesting to test direct contact as a crude cytotoxicity evaluation in further investigations that would be relevant to some clinical scenarios, for example pulpotomy indications.

In our study, both large and fine particles were found to be non-cytotoxic. In addition, the metabolic activity of cells showed a significant enhancement in the presence of particles extracts after 72 hours of incubation. Our results are in accordance with the study of Moonesi Rad et al. where the viability of cells was higher on scaffolds with boron modified BAG than without BAG [43]. Regardless of the BAG composition, in both studies the presence of BAG enhanced cells proliferation as revealed by the Alamar Blue assay. Only a few studies (like the current study) used Alamar Blue to assess pulp cells viability in contact with BAG alone [37,38]. Alamar Blue is a nontoxic reagent that allowed cell monitoring over time. It is blue-colored in its oxidized state and becomes pink colored when reduced by metabolically active cells. Crystal violet can assess and quantify cell viability, via cell adhesion, migration and spreading [39,40]. In the current study, no cytotoxic effects were observed in the presence of large and fine particles, similar to the results obtained with Wang et al. [41]. Sauro et al. 2018 demonstrated that the incorporation of zinc-doped fillers (zinc-doped bioglass) into resin-based materials enhanced bioactivity by inducing apatite precipitation, increased remineralization potential and cell differentiation [20]. However, according to Huang et al. Crystal violet staining showed an increase of cytotoxicity of ZnBAG at 20 ppm [42].

ALP is the marker of early differentiation and extracellular matrix mineralization [25]. ALP activity indicates the differentiation potential of hDPSCs in contact with BAG [42]. In the current study, both large and fine particles increased intra and extra-cellular ALP activity. Even though the composition is different between the investigated 0NaMBG and the studied BAGs in the literature, our results are in accordance with the study of Huang et al., where Zn0 glasses increased ALP activity from 1 day to 10 days [42]. Moreover, Gong et al. found that ALP activity was significantly higher in the presence of nano-58S and 45S5 groups

compared with control group after 7 days of cell culture [25]. We used confocal microscopy associated with immunostaining to assess the spreading and adhesion of cells in the presence of the experimental 0NaMBG. HDPCs in contact with large and fine particles exhibited good cytoskeletal architecture and good cell spreading. Moonesi Rad et al. used CLSM to evaluate hDPSCs spreading and differentiation on three-dimensional scaffolds containing boron modified bioactive glass nanoparticles (BG-NPs). Cells in BG-NPs containing groups were more spread and flattened on the scaffolds in comparison to the control group (scaffolds without BG-NPs). It was observed that, some cells extended processes to form cytoplasmic elongations [43]. Agrafioti et al. used confocal microscopy to observe dental pulp stem cells (DPSCs) morphology in contact with bioactive materials such as Biodentine™ and MTA [44].

Several studies showed that BAGs have the ability to form calcium deposits in contact with pulp cells. Using Alizarin red staining [35,41,42,45]. Calcium deposits can specifically be stained bright orange-red. In our study, the calcium deposition at the HDPCs interface was higher at 14 days for large particles compared with fine particles; this could be due to their higher surface area and pore volume. In the study of Wang and al. the relative calcium concentrations significantly increased in the microscale (m) and nanoscale (n) BAG groups, and were particularly higher in the nanoscale BAG compared with that in the control [41]. According to Gong and al. the density of mineralized nodules was significantly higher in the nano-58S BAG than 58S, 45S5 or control group [25]. These authors indicated that for the same BAGs composition, n-BG clusters can attract pulp cells to grow around them in cell culture and promote greater mineralization than the m-BG [41]. In our study, large particles had a higher surface area and pore volume that could explain their enhanced bioactivity.

In order to assess the odontogenic differentiation of primary cells from different origins, the markers of choice are ALP, DMP-1 and OCN. DMP-1 deemed to be one of the main non-collagenous proteins formed in the mineralized dentin matrix, it is synthesized by odontoblasts and plays an important role during early odontoblastic differentiation and at late dentin mineralization [46-49]. In our study, staining of osteopontin was revealed in the cytoplasm of cells growing in the presence of large particles extracts. While, DMP-1 was shown in both cells exposed to both large and fine particles. Huang et al. used CSLM and immunofluorescence to show that DMP-1 was localized in both cytosol and nucleus of human dental pulp cells [50], which is in agreement with our findings.

Other analyses could be used for further investigations, for example EDX spectra for calcium and phosphate content in the mineralized nodules could indicate a ratio of Ca:P similar to that of hydroxyapatite [42]. Real-time PCR could be used to assess differentiation and mineralization gene expression in the HDPCs such as Osteocalcin (OCN) gene expression [25] In our study, we used two markers: DMP-1 and osteopontin. Other markers of mineralization could also be evaluated , for example DSPP, DPP and OCN [41]. We know that larger particles had a higher surface area than fine particles; however, additional investigations could be conducted to study their different ion release rates. Despite the limitations of the present *in vitro* study and in the view of the obtained results, it is possible to validate the two suggested hypotheses: (1) both large and fine 0NaMBG particles enhanced pulp cells behavior; (2) a very high surface area of the investigated large particles had better improved the dental pulp cells behavior than the fine particles. In a recent study performed by our group, a very high surface area has been attained for the composition with highest calcium oxide which also exhibits enhanced apatite forming ability *in vitro* [17].

From a clinical perspective, using 0NaMBG particles as fillers in dental adhesives appear to be a relevant approach to explore in order to enhance the longevity of the adhesive-dentin interface [15,51] and prevent enamel demineralization [52] . The introduction of 0NaMBG as fillers in adhesive resin could replace the trapped water molecules in the resin, improve their cross linking ability and reduce the polymerization shrinkage [20,53]. Moreover, as the fillers are porous these can be functionalized with antibacterial drugs whose release could combat secondary caries. Most importantly, the reaction of MBGs with water, subsequent release of ions and the resultant formation of hydroxyapatite or calcium phosphate precipitate could protect the resin as well as the underlying collagen from hydrolytic and enzymatic degradation [54].

Conclusion

This study highlighted the superior *in vitro* biological properties of the investigated 0NaMBG particles regarding dental pulp cells. This behaviour was revealed by:

- An enhancement of metabolic activity and a non-cytotoxic potential.
- An increase of mineralization ability.

The *in vitro* obtained data raises the interesting possibility of using 0NaMBG particles as fillers in restorative materials that could be used in direct contact with dentin and/or pulp tissues. The use of bioactive materials can contribute to the preservation of natural dental tissue and/or could improve restorations lifetime, when a restorative procedure is indicated. To this end, further investigations are necessary to compare the bioactivity of 0NaMBG based materials with other available restorative materials such as calcium silicate based dental cements.

ACKNOWLEDGMENTS

The research work leading to this manuscript has partially received funding from the European Union Seventh Framework Pro-gram (FP7/2007-2013) under grant agreement n◦608197. The authors thank the "Centre d'Imagerie Quantitative *Lyon*-Est (*CIQLE*)" University Claude Bernard Lyon1 and especially Mr. Denis RESSNIKOFF for his assistance with the confocal imaging. We are also grateful to Mrs. Charlène CHEVALIER for her technical assistance with a part the experimental protocol.

REFERENCES

[1] N.B. Pitts, D.T. Zero, P.D. Marsh, K. Ekstrand, J.A. Weintraub, F. Ramos-Gomez, J. Tagami, S. Twetman, G. Tsakos, A. Ismail, Dental caries, Nat Rev Dis Primers. 3 (2017) 17030. https://doi.org/10.1038/nrdp.2017.30.

[2] P.E. Petersen, D. Bourgeois, H. Ogawa, S. Estupinan-Day, C. Ndiaye, The global burden of oral diseases and risks to oral health, Bull. World Health Organ. 83 (2005) 661–669. https://doi.org//S0042-96862005000900011.

[3] E.A. Abou Neel, A. Aljabo, A. Strange, S. Ibrahim, M. Coathup, A.M. Young, L. Bozec, V. Mudera, Demineralization-remineralization dynamics in teeth and bone, Int J Nanomedicine. 11 (2016) 4743–4763. https://doi.org/10.2147/IJN.S107624.

[4] A. Lussi, T. Jaeggi, Erosion—diagnosis and risk factors, Clin Oral Invest. 12 (2008) 5–13. https://doi.org/10.1007/s00784-007-0179-z.

[5] T. Jaeggi, A. Lussi, Prevalence, incidence and distribution of erosion, Monogr Oral Sci. 25 (2014) 55–73. https://doi.org/10.1159/000360973.

[6] N.B. Pitts, A.I. Ismail, S. Martignon, K. Ekstrand, G.V. Douglas, C. Longbottom, ICCMS Guide for Practitioners and Educators, in: 2014.

[7] F. Schwendicke, J.E. Frencken, L. Bjørndal, M. Maltz, D.J. Manton, D. Ricketts, K. Van Landuyt, A. Banerjee, G. Campus, S. Doméjean, M. Fontana, S. Leal, E. Lo, V. Machiulskiene, A. Schulte, C. Splieth, A.F. Zandona, N.P.T. Innes, Managing Carious Lesions: Consensus Recommendations on Carious Tissue Removal, Adv. Dent. Res. 28 (2016) 58–67.

[8] European Society of Endodontology (ESE) developed by:, H.F. Duncan, K.M. Galler, P.L. Tomson, S. Simon, I. El-Karim, R. Kundzina, G. Krastl, T. Dammaschke, H. Fransson, M. Markvart, M. Zehnder, L. Bjørndal, European Society of Endodontology position statement: Management of deep caries and the exposed pulp, Int Endod J. 52 (2019) 923–934. https://doi.org/10.1111/iej.13080.

[9] D. Hashem, F. Mannocci, S. Patel, A. Manoharan, J.E. Brown, T.F. Watson, A. Banerjee, Clinical and radiographic assessment of the efficacy of calcium silicate indirect pulp capping: a randomized controlled clinical trial, J. Dent. Res. 94 (2015) 562–568. https://doi.org/10.1177/0022034515571415.

[10] F. Schwendicke, A. Al-Abdi, A. Pascual Moscardó, A. Ferrando Cascales, S. Sauro, Remineralization effects of conventional and experimental ion-releasing materials in chemically or bacterially-induced dentin caries lesions, Dent Mater. 35 (2019) 772–779. https://doi.org/10.1016/j.dental.2019.02.021.

[11] F.R. Tay, D.H. Pashley, Biomimetic remineralization of resin-bonded acid-etched dentin, J. Dent. Res. 88 (2009) 719–724. https://doi.org/10.1177/0022034509341826.

[12] L.L. Hench, The story of Bioglass, J Mater Sci Mater Med. 17 (2006) 967–978. https://doi.org/10.1007/s10856-006-0432-z.

[13] S.J. Graumann, M.L. Sensat, J.L. Stoltenberg, Air polishing: a review of current literature, J Dent Hyg. 87 (2013) 173–180.
[14] A.A. Taha, M.P. Patel, R.G. Hill, P.S. Fleming, The effect of bioactive glasses on enamel remineralization: A systematic review, J Dent. 67 (2017) 9–17. https://doi.org/10.1016/j.jdent.2017.09.007.
[15] D. Fernando, N. Attik, N. Pradelle-Plasse, P. Jackson, B. Grosgogeat, P. Colon, Bioactive glass for dentin remineralization: A systematic review, Mater Sci Eng C Mater Biol Appl. 76 (2017) 1369–1377. https://doi.org/10.1016/j.msec.2017.03.083.
[16] A. Banerjee, M. Hajatdoost-Sani, S. Farrell, I. Thompson, A clinical evaluation and comparison of bioactive glass and sodium bicarbonate air-polishing powders, Journal of Dentistry. 38 (2010) 475-479. https://doi.org/10.1016/j.jdent.2010.03.001.
[17] D. Fernando, N. Attik, M. Cresswell, I. Mokbel, N. Pradelle-Plasse, P. Jackson, B. Grosgogeat, P. Colon, Influence of network modifiers in an acetate based sol-gel bioactive glass system, Microporous and Mesoporous Materials. 257 (2018) 99–109. https://doi.org/10.1016/j.micromeso.2017.08.029.
[18] D. Fernando, P. Colon, M. Cresswell, C. Journet, N. Pradelle-Plasse, P. Jackson, B. Grosgogeat, N. Attik, The influence of precursor addition order on the porosity of sol-gel bioactive glasses, Dent Mater. 34 (2018) 1323–1330. https://doi.org/10.1016/j.dental.2018.06.003.
[19] B. Oguntebi, A. Clark, J. Wilson, Pulp capping with Bioglass and autologous demineralized dentin in miniature swine, J. Dent. Res. 72 (1993) 484–489. https://doi.org/10.1177/00220345930720020301.
[20] S. Sauro, A. Babbar, B. Gharibi, V.P. Feitosa, R.M. Carvalho, L.K. Azevedo Rodrigues, A. Banerjee, T. Watson, Cellular differentiation, bioactive and mechanical properties of experimental light-curing pulp protection materials, Dent Mater. 34 (2018) 868–878. https://doi.org/10.1016/j.dental.2018.02.008.
[21] L.B. Mestieri, A.L. Gomes-Cornélio, E.M. Rodrigues, L.P. Salles, R. Bosso-Martelo, J.M. Guerreiro-Tanomaru, M. Tanomaru-Filho, Biocompatibility and bioactivity of calcium silicate-based endodontic sealers in human dental pulp cells, J Appl Oral Sci. 23 (2015) 467–471. https://doi.org/10.1590/1678-775720150170.
[22] K.C. da S. Modena, L.C. Casas-Apayco, M.T. Atta, C.A. de S. Costa, J. Hebling, C.R. Sipert, M.F. de L. Navarro, C.F. Santos, Cytotoxicity and biocompatibility of direct and indirect pulp capping materials, J Appl Oral Sci. 17 (2009) 544–554. https://doi.org/10.1590/S1678-77572009000600002.
[23] M.L. Couble, J.C. Farges, F. Bleicher, B. Perrat-Mabillon, M. Boudeulle, H. Magloire, Odontoblast differentiation of human dental pulp cells in explant cultures, Calcif. Tissue Int. 66 (2000) 129–138. https://doi.org/10.1007/pl00005833.
[24] S.M. Carvalho, A.A.R. Oliveira, C.A. Jardim, C.B.S. Melo, D.A. Gomes, M. de Fátima Leite, M.M. Pereira, Characterization and induction of cementoblast cell proliferation by bioactive glass nanoparticles, J Tissue Eng Regen Med. 6 (2012) 813–821. https://doi.org/10.1002/term.488.
[25] W. Gong, Z. Huang, Y. Dong, Y. Gan, S. Li, X. Gao, X. Chen, Ionic extraction of a novel nano-sized bioactive glass enhances differentiation and mineralization of human dental pulp cells, J Endod. 40 (2014) 83–88. https://doi.org/10.1016/j.joen.2013.08.018.
[26] B.P. McNicholl, J.W. McGrath, J.P. Quinn, Development and application of a resazurin-based biomass activity test for activated sludge plant management, Water Res. 41 (2007) 127–133. https://doi.org/10.1016/j.watres.2006.10.002.

[27] E. Patel, P. Pradeep, P. Kumar, Y.E. Choonara, V. Pillay, Oroactive dental biomaterials and their use in endodontic therapy, Journal of Biomedical Materials Research Part B: Applied Biomaterials. 108 (2020) 201–212. https://doi.org/10.1002/jbm.b.34379.
[28] S. Ferraris, S. Yamaguchi, N. Barbani, M. Cazzola, C. Cristallini, M. Miola, E. Vernè, S. Spriano, Bioactive materials: In vitro investigation of different mechanisms of hydroxyapatite precipitation, Acta Biomater. 102 (2020) 468–480. https://doi.org/10.1016/j.actbio.2019.11.024.
[29] I. Izquierdo-Barba, M. Vallet-Regí, Mesoporous Bioactive Glasses: Relevance of Their Porous Structure Compared to that of Classical Bioglasses, Biomedical Glasses. 1 (2015). https://doi.org/10.1515/bglass-2015-0014.
[30] X. Yan, C. Yu, X. Zhou, J. Tang, D. Zhao, Highly ordered mesoporous bioactive glasses with superior in vitro bone-forming bioactivities, Angew. Chem. Int. Ed. Engl. 43 (2004) 5980–5984. https://doi.org/10.1002/anie.200460598.
[31] J. Camilleri, T. Arias Moliz, A. Bettencourt, J. Costa, F. Martins, D. Rabadijeva, D. Rodriguez, L. Visai, C. Combes, C. Farrugia, P. Koidis, C. Neves, Standardization of antimicrobial testing of dental devices, Dental Materials. 36 (2020) e59–e73. https://doi.org/10.1016/j.dental.2019.12.006.
[32] the International Organization for Standardization, ISO 10993-5:2009 Biological evaluation of medical devices - part 5: tests for in vitro cytotoxicity, ISO. (2009). https://www.iso.org/obp/ui/fr/#iso:std:iso:10993:-5:ed-3:v1:en (accessed January 18, 2020).
[33] E.S. Gjorgievska, J.W. Nicholson, S.M. Apostolska, N.J. Coleman, S.E. Booth, I.J. Slipper, M.I. Mladenov, Interfacial properties of three different bioactive dentine substitutes, Microsc. Microanal. 19 (2013) 1450–1457. https://doi.org/10.1017/S1431927613013573.
[34] S. Zhang, D. Ye, L. Ma, Y. Ren, R.T. Dirksen, X. Liu, Purinergic Signaling Modulates Survival/Proliferation of Human Dental Pulp Stem Cells, J Dent Res. 98 (2019) 242–249. https://doi.org/10.1177/0022034518807920.
[35] W.-J. Bae, K.-S. Min, J.-J. Kim, J.-J. Kim, H.-W. Kim, E.-C. Kim, Odontogenic responses of human dental pulp cells to collagen/nanobioactive glass nanocomposites, Dent Mater. 28 (2012) 1271–1279. https://doi.org/10.1016/j.dental.2012.09.011.
[36] T.Y. Saw, T. Cao, A.U.J. Yap, M.M. Lee Ng, Tooth slice organ culture and established cell line culture models for cytotoxicity assessment of dental materials, Toxicol In Vitro. 19 (2005) 145–154. https://doi.org/10.1016/j.tiv.2004.08.006.
[37] S. Gholami, S. Labbaf, A.B. Houreh, H.-K. Ting, J.R. Jones, M.-H.N. Esfahani, Long term effects of bioactive glass particulates on dental pulp stem cells in vitro, Biomedical Glasses. 3 (2017) 96–103. https://doi.org/10.1515/bglass-2017-0009.
[38] A.B. Houreh, S. Labbaf, H.-K. Ting, F. Ejeian, J.R. Jones, M.-H.N. Esfahani, Influence of calcium and phosphorus release from bioactive glasses on viability and differentiation of dental pulp stem cells, J. Mater. Sci. 52 (2017) 8928–8941. https://doi.org/10.1007/s10853-017-0946-4.
[39] M.A. Gharaei, Y. Xue, K. Mustafa, S.A. Lie, I. Fristad, Human dental pulp stromal cell conditioned medium alters endothelial cell behavior, Stem Cell Res Ther. 9 (2018). https://doi.org/10.1186/s13287-018-0815-3.
[40] C. Strojny, M. Boyle, A. Bartholomew, P. Sundivakkam, S. Alapati, Interferon Gamma-treated Dental Pulp Stem Cells Promote Human Mesenchymal Stem Cell Migration In Vitro, J Endod. 41 (2015) 1259–1264. https://doi.org/10.1016/j.joen.2015.02.018.
[41] S. Wang, X. Gao, W. Gong, Z. Zhang, X. Chen, Y. Dong, Odontogenic differentiation

and dentin formation of dental pulp cells under nanobioactive glass induction, Acta Biomater. 10 (2014) 2792–2803. https://doi.org/10.1016/j.actbio.2014.02.013.
[42] M. Huang, R.G. Hill, S.C.F. Rawlinson, Zinc bioglasses regulate mineralization in human dental pulp stem cells, Dent Mater. 33 (2017) 543–552. https://doi.org/10.1016/j.dental.2017.03.011.
[43] R. Moonesi Rad, D. Atila, E.E. Akgün, Z. Evis, D. Keskin, A. Tezcaner, Evaluation of human dental pulp stem cells behavior on a novel nanobiocomposite scaffold prepared for regenerative endodontics, Mater Sci Eng C Mater Biol Appl. 100 (2019) 928–948. https://doi.org/10.1016/j.msec.2019.03.022.
[44] A. Agrafioti, V. Taraslia, V. Chrepa, S. Lymperi, P. Panopoulos, E. Anastasiadou, E.G. Kontakiotis, Interaction of dental pulp stem cells with Biodentine and MTA after exposure to different environments, J Appl Oral Sci. 24 (2016) 481–486. https://doi.org/10.1590/1678-775720160099.
[45] S. Wang, Q. Hu, X. Gao, Y. Dong, Characteristics and Effects on Dental Pulp Cells of a Polycaprolactone/Submicron Bioactive Glass Composite Scaffold, J Endod. 42 (2016) 1070–1075. https://doi.org/10.1016/j.joen.2016.04.023.
[46] P.A. Baldión, M.L. Velandia-Romero, J.E. Castellanos, Odontoblast-Like Cells Differentiated from Dental Pulp Stem Cells Retain Their Phenotype after Subcultivation, Int J Cell Biol. 2018 (2018) 6853189. https://doi.org/10.1155/2018/6853189.
[47] J.-H. Lee, M.-S. Kang, C. Mahapatra, H.-W. Kim, Effect of Aminated Mesoporous Bioactive Glass Nanoparticles on the Differentiation of Dental Pulp Stem Cells, PLoS ONE. 11 (2016) e0150727. https://doi.org/10.1371/journal.pone.0150727.
[48] S. Tian, J. Wang, F. Dong, N. Du, W. Li, P. Song, Y. Liu, Concentrated Growth Factor Promotes Dental Pulp Cells Proliferation and Mineralization and Facilitates Recovery of Dental Pulp Tissue, Med. Sci. Monit. 25 (2019) 10016–10028. https://doi.org/10.12659/MSM.919316.
[49] V.K. Gopinath, S. Soumya, M.N. Jayakumar, Osteogenic and odontogenic differentiation potential of dental pulp stem cells isolated from inflamed dental pulp tissues (I-DPSCs) by two different methods, Acta Odontol. Scand. 78 (2020) 281–289. https://doi.org/10.1080/00016357.2019.1702716.
[50] M. Huang, R.G. Hill, S.C.F. Rawlinson, Strontium (Sr) elicits odontogenic differentiation of human dental pulp stem cells (hDPSCs): A therapeutic role for Sr in dentine repair?, Acta Biomater. 38 (2016) 201–211. https://doi.org/10.1016/j.actbio.2016.04.037.
[51] A.L.M. Ubaldini, R.C. Pascotto, F. Sato, V.O. Soares, M.L. Baesso, Mechanical and Chemical Changes in the Adhesive-Dentin Interface after Remineralization, J Adhes Dent. 22 (2020) 297–309. https://doi.org/10.3290/j.jad.a44553.
[52] A. Alamri, Z. Salloot, A. Alshaia, M.S. Ibrahim, The Effect of Bioactive Glass-Enhanced Orthodontic Bonding Resins on Prevention of Demineralization: A Systematic Review, Molecules. 25 (2020). https://doi.org/10.3390/molecules25112495
[53] N. Kohda, M. Iijima, K. Kawaguchi, H. Toshima, T. Muguruma, K. Endo, I. Mizoguchi, Inhibition of enamel demineralization and bond-strength properties of bioactive glass containing 4-META/MMA-TBB-based resin adhesive, Eur. J. Oral Sci. 123 (2015) 202–207. https://doi.org/10.1111/eos.12187.
[54] R. Osorio, M. Yamauti, S. Sauro, T.F. Watson, M. Toledano, Experimental resin cements containing bioactive fillers reduce matrix metalloproteinase-mediated dentin collagen degradation, J Endod. 38 (2012) 1227–1232. https://doi.org/10.1016/j.joen.2012.05.011.

Figure captions

Fig. 1. Metabolic activity of human dental pulp cells interfaced with MBGs extracts after 24, 48 and 72h. Data re mean ±SD of 3 independent experiments (n=9). *p<0.05 compared with control cells

Fig. 2 - ALP activity of hDP cells following MBGs particles treatment. (A) ALP intra cellular-activity (B) ALP extra-cellular activity. Data are mean ±SD of 3 independent experiments (n=9). *p<0.05 compared with control cells

Fig. 3 - Crystal violet staining on control cells (A), indirect contact with fine particles (B) and large particles (C).

Fig. 4 - Percentage of cytotoxicity detected by Crystal violet quantification. Data are mean ±SD of 3 independent experiments (n=9). No significant difference compared with control cells

Fig. 5 - hDPCs morphology and spreading by confocal microscopy (A) control cells, (B) fine particles and (C) large particles. Actin cytoskeleton in green fluorescence and nuclei in red fluorescence (Scale bars = 20 μm).

Fig. 6 - Quantification of calcium deposition of hDP cells interfaced with MBGs particles using Alizarin Red S staining. Data are mean ±SD of 3 independent experiments (n=9). *p<0.05 compared with control cells

Fig. 7 - Representative images of Alizarin Red S staining of hDP cells. Cells were cultured in (A) culture medium, (B) fine particles extracts and (C) large particles extracts media (Scale bars = 100 μm).

Fig. 8 - Immunofluorsescence staining of osteopontin in hDPs cells cultured on indirect contact of particles. Control cells (A), fine particles medium (B) and large particles medium (C). Osteopontin in red and cell nuclei in blue (Scale bars = 30 μm).

Fig. 9 - Immunofluorescence staining of DMP-1 in hDPs cells cultured on indirect contact of particles. Control cells (A), fine particles medium (B) and large particles medium (C). DMP1 in red fluorescence and cell nuclei in blue fluorescence (Scale bars = 50 μm).

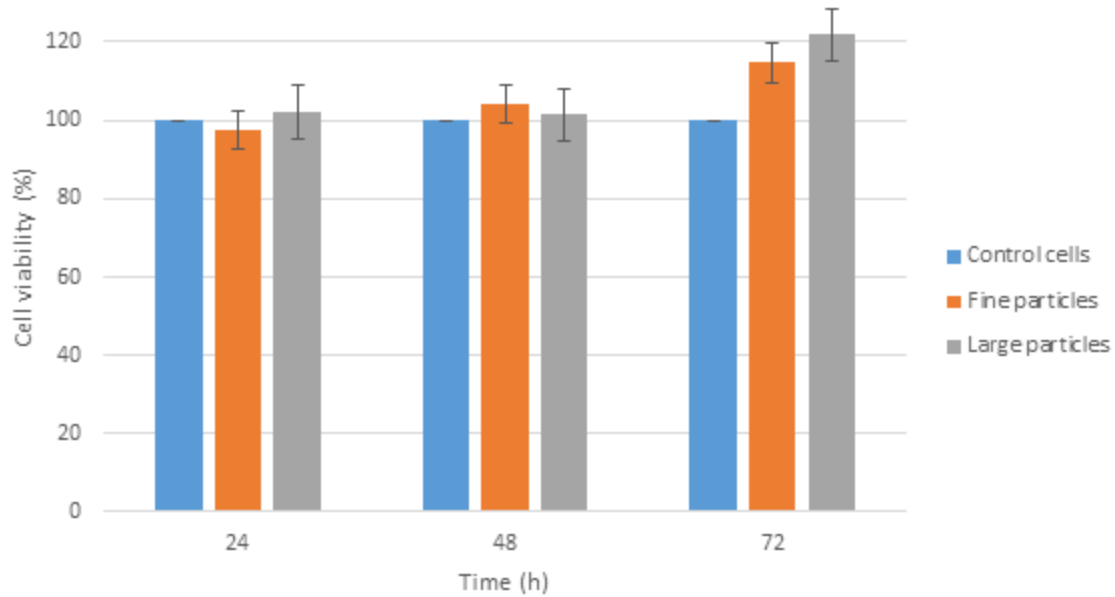
120
100
80
60
40
20
0
Cell viability (%)
24
48
72
Time (h)
Control cells
Fine particles
Large particles

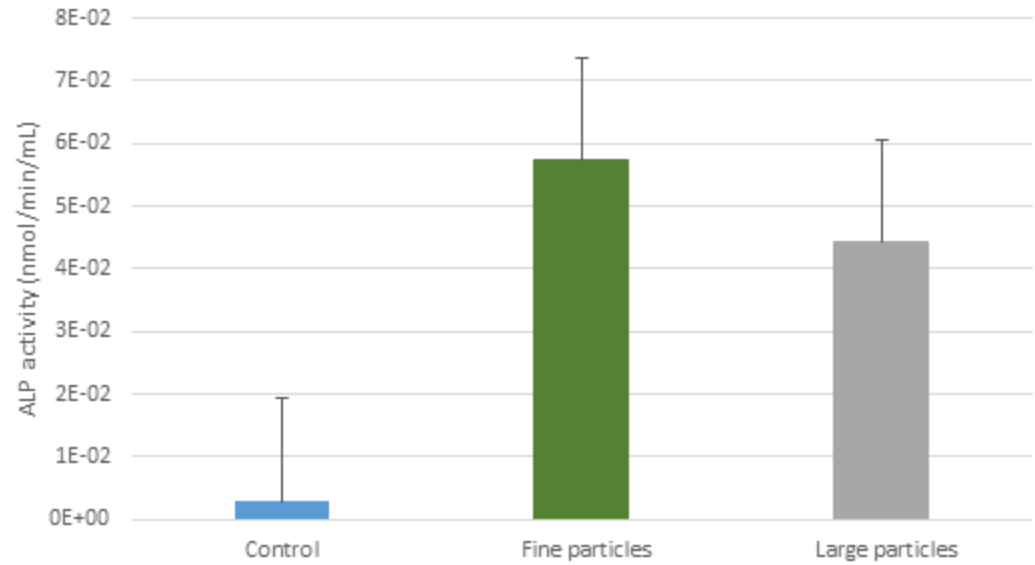
8E-02
7E-02
6E-02
5E-02
4E-02
3E-02
2E-02
1E-02
0E+00
ALP activity (nmol/min/mL)
Control
Fine particles
Large particles

A

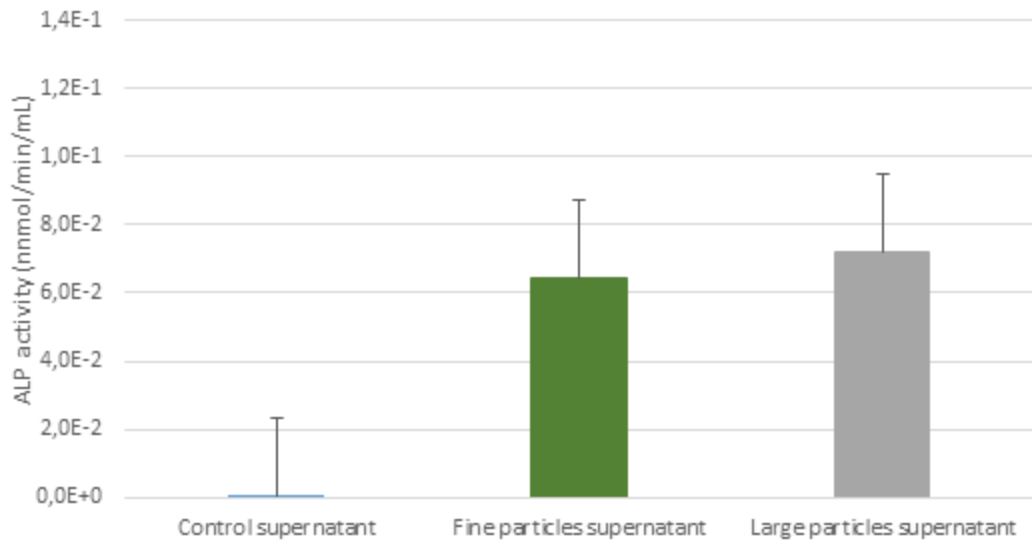
1,4E-1
1,2E-1
1,0E-1
8,0E-2
6,0E-2
4,0E-2
2,0E-2
0,0E+0
ALP activity (nnmol/min/mL)
Control supernatant
Fine particles supernatant
Large particles supernatant

B

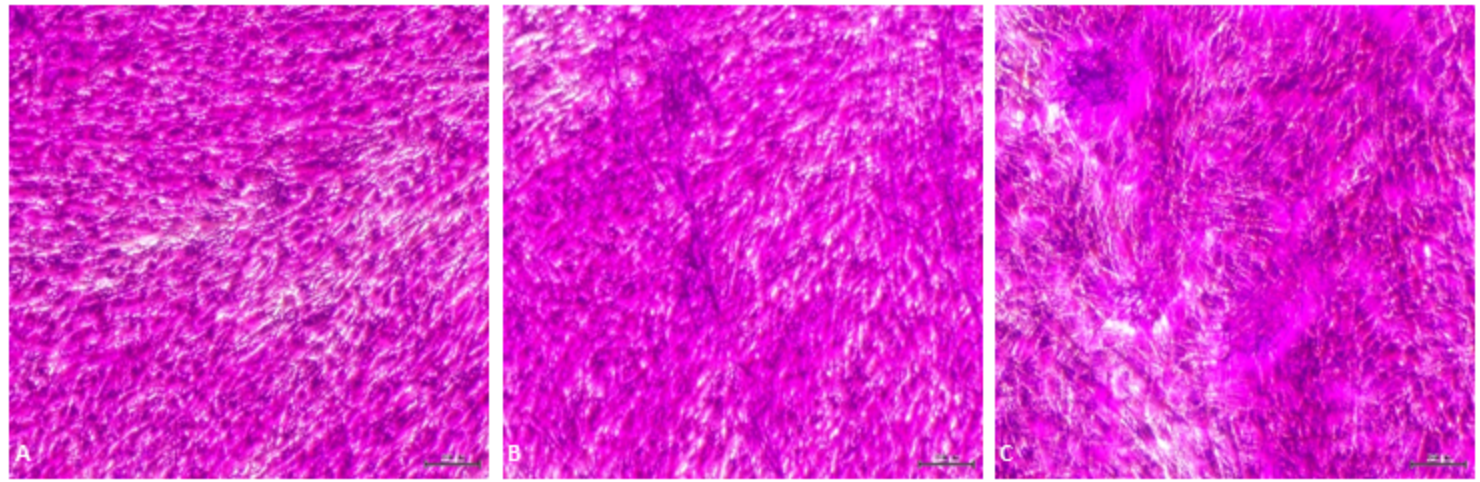
A
B
C

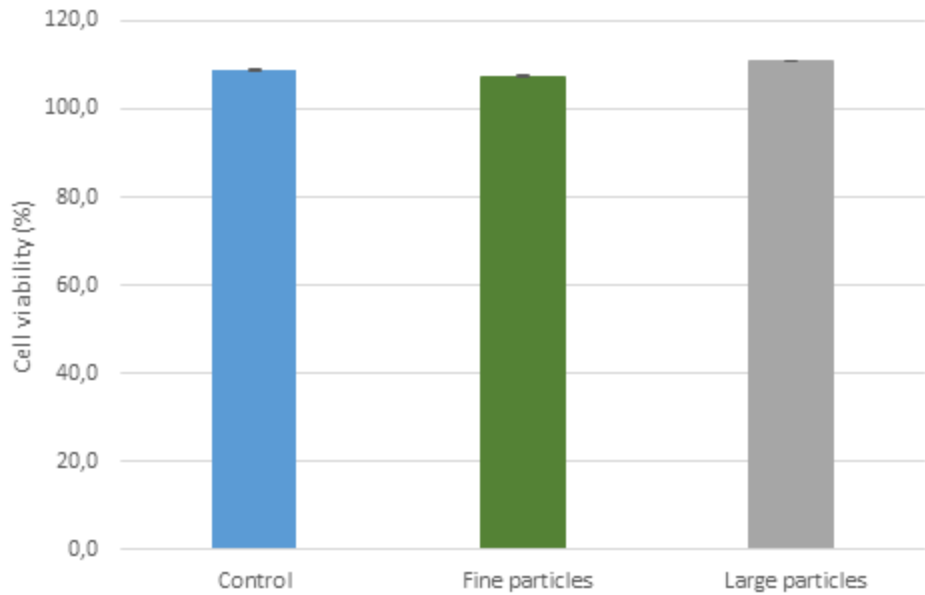
120,0
100,0
80,0
60,0
40,0
20,0
0,0
Cell viability (%)
Control
Fine particles
Large particles

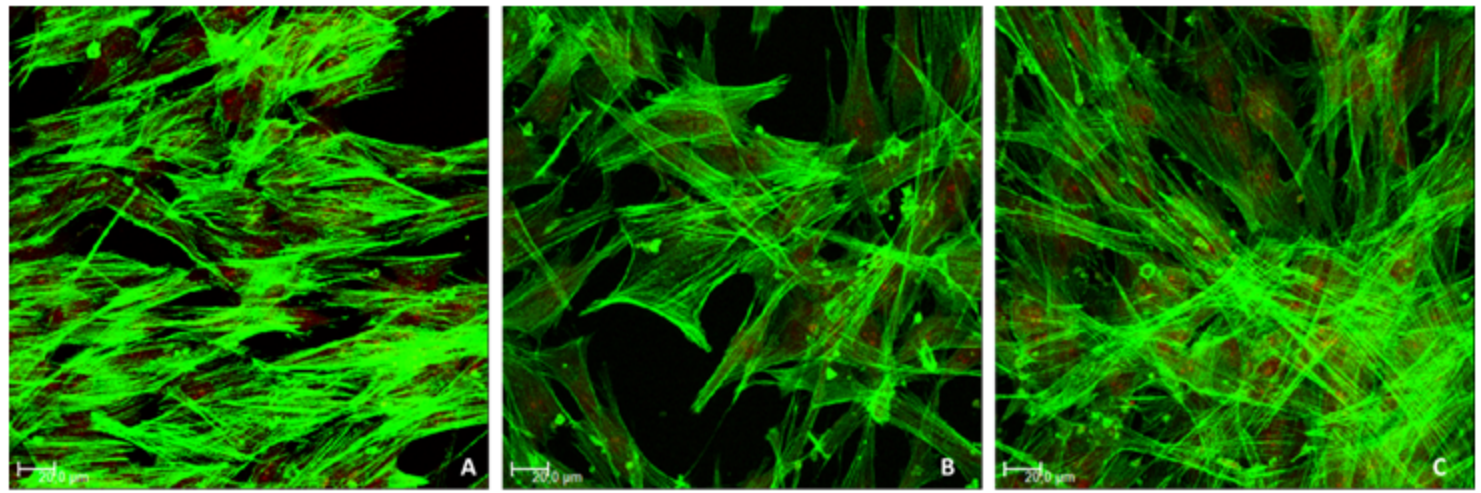
200 µm
A
200 µm
B
200 µm
C

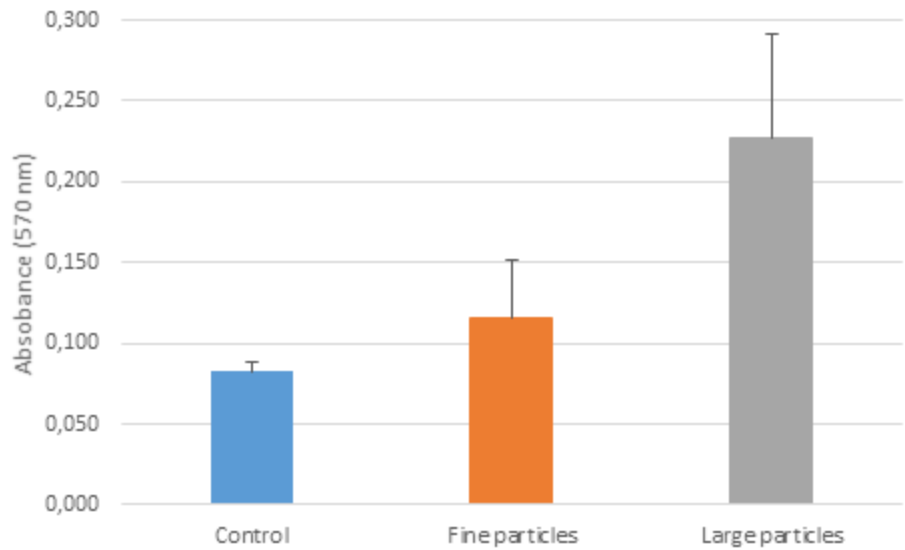
0,300
0,250
0,200
0,150
0,100
0,050
0,000
Absobance (570 nm)
Control
Fine particles
Large particles

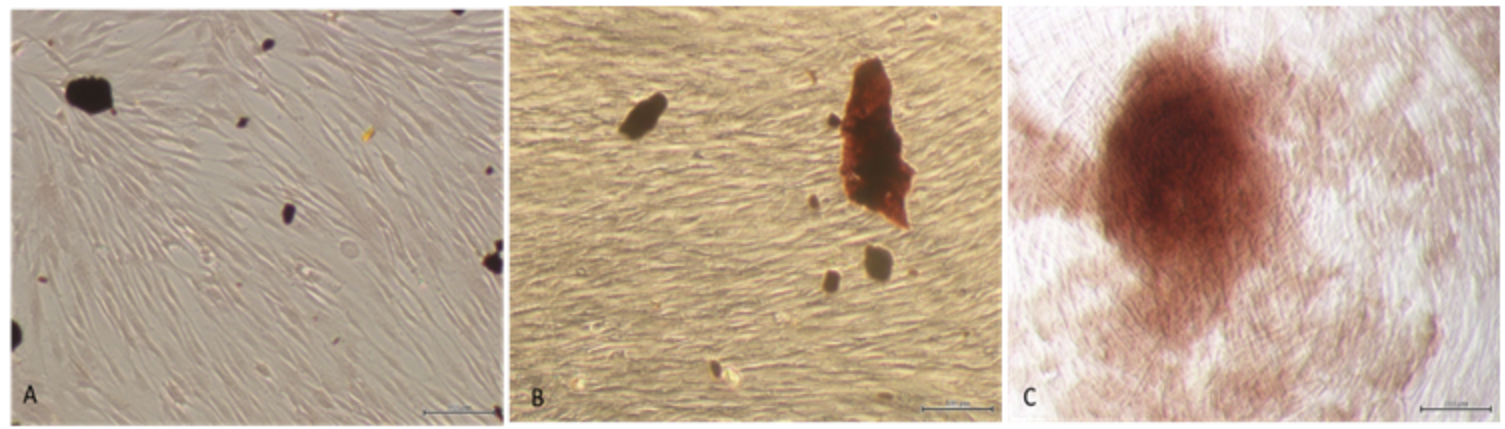
A
B
C

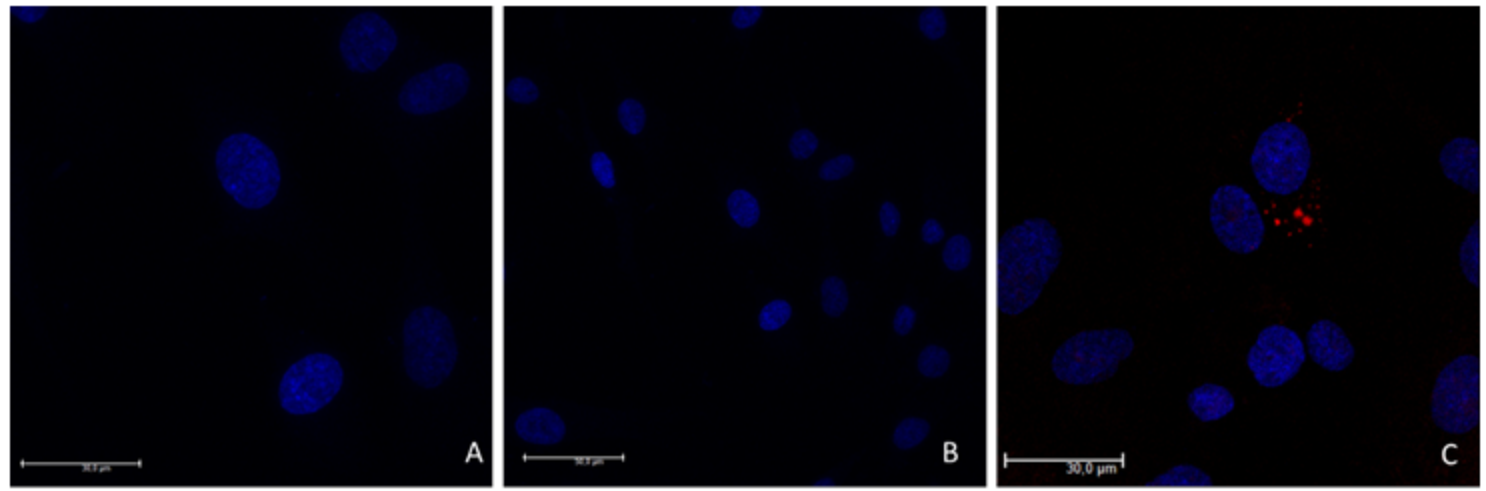
A
B
C
30,0 µm

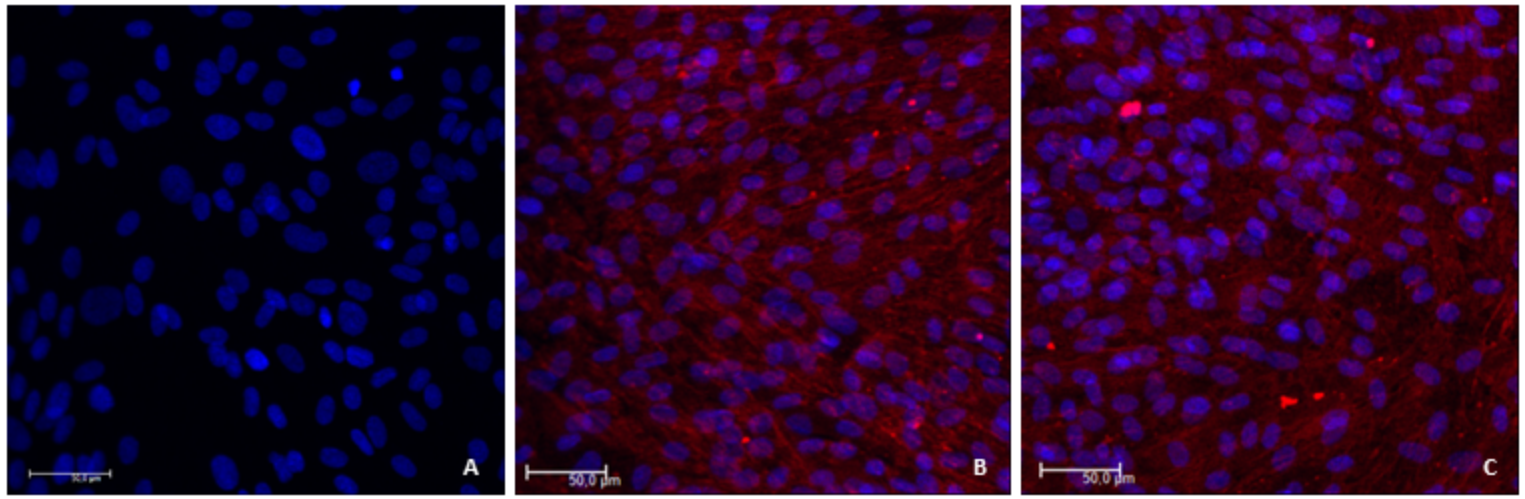
A
50,0 µm
B
50,0 µm
C

Table 1 – 0NaMBG particles size, pore volume and pore size data

Samples	SURFACE AREA (m^2g^{-1})	PORE VOLUME (cm^3g^{-1})	PORE SIZE (nm)
Larges particles	171	0.120	9.4
Fine Particles	422	0.421	3.6